Title
Identification of microseismic attributes through spectral analysis

ISBN
9781613994337

Authors
Nava, MJ
Rector, JW
Zhang, Z

Publication Date
2015

DOI
10.2118/178636-ms

Peer reviewed

Identification of Microseismic Attributes Through Spectral Analysis

Michael J. Nava, James W. Rector, and Zhishuai Zhang, University of California, Berkeley

Summary

The canonical monitoring geometry for hydraulic fracturing processes consists of a horizontal treatment well and a roughly parallel observation well that contains an array of acoustic sensors. This is a cost-effective method because it allows for relatively high-resolution monitoring with a low number of cross-well geophones. However, there is a significant drawback with this type of monitoring technique. Specifically, moment tensor inversion suffers based on a small solid angle, which is due to limited aperture. While the current literature suggests that additional monitoring wells are necessary to gain a better understanding of microseismic attributes, that solution is accompanied by a much higher cost. Another proposed solution to this problem is through the use of large surface monitoring arrays; however, what is gained in azimuthal coverage is often lost due to the introduction of significant noise. In an effort to minimize overall cost and improve the understanding of microseismic source mechanisms with this basic monitoring geometry, we propose a new approach that relies primarily on spectral analysis.

Though careful exploration in the frequency domain, specific parameters like center frequency and bandwidth, combined with knowledge of pumping parameters, lead to inferences regarding microseismic source mechanisms that would be otherwise unavailable. The benefits of this approach are significant due to the fact that an understanding of microseismic source mechanisms can lead to a greater awareness of new fractures and associated permeability of the fracture network. Moreover, circumventing the limitations accompanied by the traditional survey geometry due to limited aperture while minimizing overall cost can have a significant impact on the viability of new hydraulic fracturing processes.

Introduction

Typical hydraulic fracturing processes are performed using horizontally drilled boreholes, called treatment wells, located within a zone of interest in order to capture hydrocarbon-rich material like oil and natural gas. Once the treatment well is drilled, fracturing fluid, which is typically water and sand, or proppant, is pumped at high pressure in order to cause fractures within the treatment zone at depth. Once the pumps are turned off and the pressure drops, the proppant keeps newly created fractures open in order to increase porosity and permeability within the zone of interest. The fracturing fluid is pumped back out of the treatment well along with gas and other hydrocarbon-rich material.

One of the more cost-effective methods of monitoring these hydraulic fracturing processes is to drill a second horizontal borehole, the observation well, parallel and roughly at the same depth as the treatment well. This well is used to deploy an array of acoustic sensors, or geophones, in

order to capture the acoustic emissions from nearby microseismic events. This is a cost-effective method because after the first treatment well has been completed, the observation well can then be used to produce natural gas and other hydrocarbons as well. There are certainly advantages to this approach given that a greater area of the pay zone can be produced since the horizontal treatment well spans a much greater distance than a vertical wellbore. For example, if a shale layer were 250 ft thick, then a vertical well would only have a pay zone of 250 ft. Conversely, a horizontal well can have, as is the case in this specific hydraulic fracturing process, a pay zone of 5,600 ft.

Despite these significant advantages, there are also limitations imposed by this approach. For example, it is more difficult to locate microseismic events due to the orientation of geophones. Specifically, where vertical monitoring arrays can more accurately constrain depth and subsequent location of an event, horizontal monitoring arrays rely on hodogram angle of inclination to determine the depth of an event, which increases uncertainty (Maxwell 2014). Furthermore, the location and orientation of the observation well is determined based on balancing two conditions: where good recording of events can occur, but also, and likely more importantly, where the most gas can be produced from the well.

One of the principle difficulties in microseismic monitoring of hydraulic fracturing processes is a limitation stemming directly from the survey geometry. Specifically, due to the parallel orientation of the observation and treatment wells, there inherently exists a limitation in the azimuthal coverage of microseismic monitoring sensors; this is referred to as a limited aperture. As a result of this condition, significant challenges arise. For example, moment tensor inversion is extremely difficult to perform due to the small solid angle (Du et al. 2011; Vavrycuk 2007). As such, there is a higher level of uncertainty regarding source mechanism. Additionally, a common source of error that is more likely to occur in crosswell monitoring comes from ringing that can be attributed to tubes waves at resonant frequencies (Bainbridge et al. 1996; Daley 2003). The main cause of this phenomenon is poor coupling between geophones and the observation well. Current research suggests that additional monitoring wells are required to circumvent the limited aperture problem; however, this is a cost prohibitive option. As such, we propose the use of spectral analysis as a means to overcome the limited aperture problem and find insight regarding the microseismic events.

Hydraulic Fracturing Microseismic Monitoring Overview

The hydraulic fracturing project was performed in Susquehanna County, Pennsylvania in the Marcellus shale formation. Two horizontal boreholes were drilled to complete the hydraulic fracturing process. One borehole was used as a treatment well and was pressurized with the intention of causing fractures in the treatment zone. The other borehole was used as a monitoring well and contained an array of geophones. The treatment well was approximately 5,600 ft long and the observation well was slightly shorter at approximately 4,400 ft in length. The average

distance between the treatment well and the observation well was approximately 720 ft. The microseismic monitoring sensors employed to capture the acoustic energy of the project were miniaturized multi-component borehole sonde strings consisting of eleven geophones each spaced approximately 50 ft from one other. While it is certainly preferable to clamp, or lock into place, the geophones in a crosswell monitoring configuration, the geophones in this project were not clamped. As such, the weight of the monitoring instrument was the only coupling force adhering the tool to the borehole casing.

The main focus of monitoring this hydraulic fracturing project was to investigate the potential of increasing stimulation efficiency by only changing operational constraints such as pump rate. As such, a variable pump rate design was implemented in nine of the eighteen stages that were completed in the overall project. Pumping parameters were monitored in an effort to correlate increased gas production with those stages implementing the varied rate design. Preliminary findings, however, are inconclusive as to whether a variable rate design of pumping stages leads to an increase in gas production. Despite this, the hydraulic fracturing project was successful in producing hydrocarbon from the treatment well.

In an effort to reduce viewing distance while fracturing each of the eighteen stage the geophone array was moved six times throughout the hydraulic fracturing project, shown in Figure 1. A listing of the stages associated with each geophone array location can be seen in Table 1. This decision has both advantages and disadvantages. For instance, with a reduced viewing distance, signal-to-noise is typically improved as a result of diminished scattering and attenuation effects; however, there is also a dramatic reduction in azimuthal coverage. As such, there is a tradeoff between reduced noise and a reduced ability to determine specific source mechanisms through traditional means.

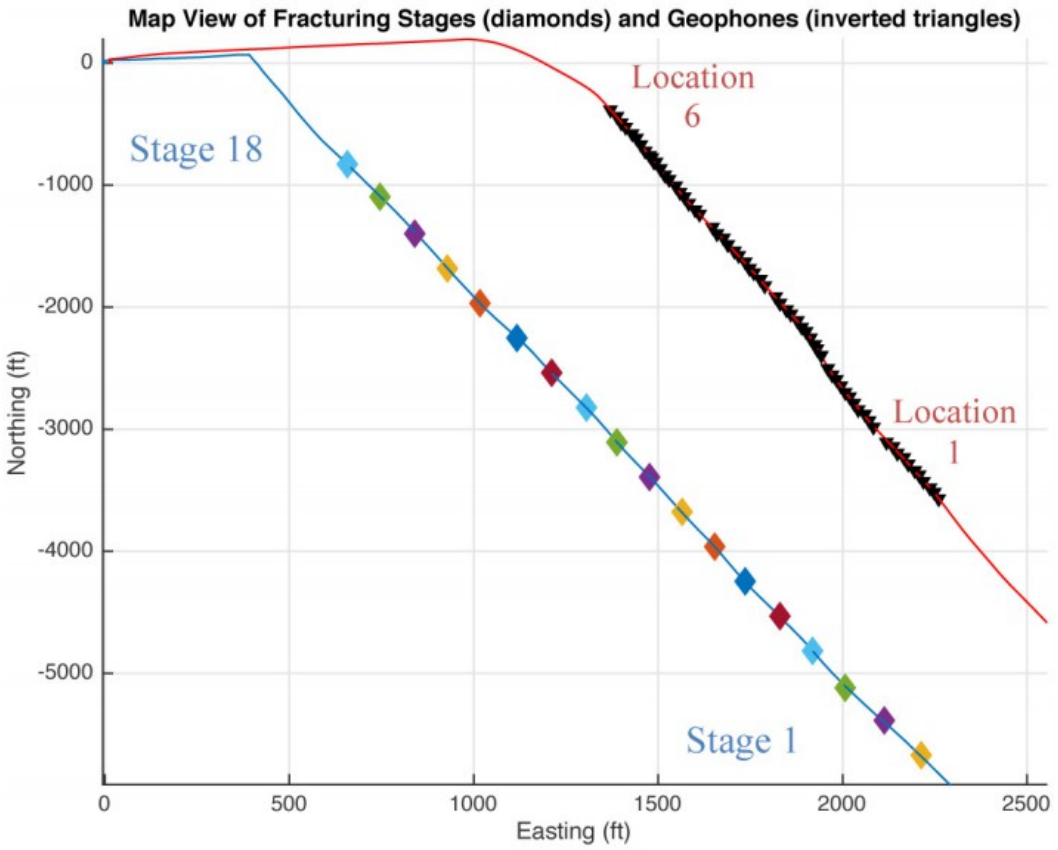

Figure 1—Map view of hydraulic fracturing process in the Marcellus Shale. Relative distances are given in the Easting and Northing directions. Blue line represents the treatment well and the red line indicates the observation well. Multi-colored diamonds represent the locations of perforation shots for each of the eighteen stages. Stage one is at the toe of the well and stage eighteen is at the heel of the well. Black inverted triangles represent the six locations of the geophone array.

Table 1—Description of geophone movement throughout hy- draulic fracturing project

Hydraulic Fracturing Stage	Geophone Array Location
1 – 9	1
10 – 11	2
12 – 13	3
14 – 15	4
16 – 17	5
18	6

Methods

Preliminary analysis of raw microseismic data showed the presence of large amplitude resonances at high frequencies. Given the fact that the three-component geophones used in the monitoring array were not clamped to the monitoring well casing, these high frequency phenomena are likely caused by tube waves propagating through the borehole (Gaiser et al. 1988). In order to mitigate this artifact, a number of processing techniques were implemented.

For example, low pass and band pass Butterworth filters were applied to the raw data. Additionally, a location-based noise characterization and removal schema was developed. This location-based approach is important since the geophone array was relocated multiple times throughout the hydraulic fracturing process. As such, the noise signature changes with each move of the array due to inconsistencies in source-receiver pathways, orientation of individual geophones, and heterogeneity of material between geophone and wellbore casing. This approach considered the root mean square (rms) value of each of the eleven geophones in the array for all events and then determined an average rms for events occurring at each location of the array. Dividing the raw data by these scalar values produced a much more readable signal, free of these large amplitude ringing artifacts. Figure 2 shows an example of the presence of a large amplitude artifact believed to be a tube wave.

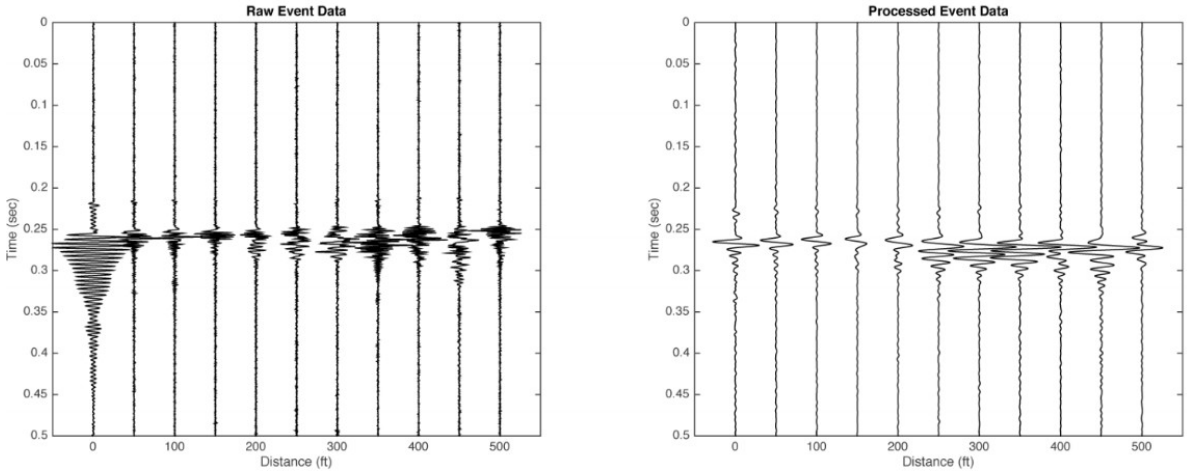

Figure 2—Comparison of raw data (left) showing the presence of a large amplitude artifact, likely caused by interference from a tube wave propagating through the observation well.

Concurrently, a microseismic analysis toolkit was developed in Matlab that enables the user to interactively navigate multiple views of the data. The first view shows seismograms of raw and processed data and the second view shows the event locations as a function of various parameters. The main purpose and most impactful aspect of this microseismic analysis toolkit, however, is the final view, which enables the user to visualize and interpret events in the spectral domain. In order to display event spectra in a readable manner, a number of processing steps were performed. First, it was necessary to window the compressional and shear wave arrivals. In order to accomplish this, the first breaks of the waveforms were automatically detected and also manually picked. After comparing both of these results, the most coherent arrival times were chosen. From here, a 100 ms Tukey window (Equation 1), or tapered cosine window, was empirically chosen and applied to the data in order to capture the relevant frequency content of both the compressional and shear waveforms. Once the waveforms to be investigated were isolated, the average spectra were calculated. Since there are eleven geophones in the array, a Fourier Transform was performed on all traces, which yielded eleven spectral responses. These

responses were then averaged in order to give an indication of frequency content on a total event basis.

$$w(x) = \begin{cases} \frac{1}{2}\left\{1 + cos\left(\frac{2\pi}{r}\left[x - \frac{r}{2}\right]\right)\right\} & , \quad 0 \leq x < \frac{r}{2} \\ 1 & , \quad \frac{r}{2} \leq x < 1 - \frac{r}{2} \\ \frac{1}{2}\left\{1 + cos\left(\frac{2\pi}{r}\left[x - 1 + \frac{r}{2}\right]\right)\right\} & , \quad 1 - \frac{r}{2} \leq x < 1 \end{cases} \tag{1}$$

After finding the average spectral response per event for the compressional wave and shear wave independently, a combined window was created that captures both the compressional and the shear waves for each event. With three main data fields to be investigated - windowed compressional wave, windowed shear wave, and a combined window - we are now able to begin classifying event characteristics based on spectral analysis.

Center Frequency

In an effort to categorize and characterize microseismic events through spectral analysis, the center frequency of each event was evaluated. In order to accomplish this, the centroid method of signal analysis was applied (Bracewell 1965). Modeling the event spectra as a distributed load and determining the first moment, or centroid, of the signal enables the identification of the frequencies at which the greatest amount of signal energy is located. This approach yields the abscissa x , which is synonymous with the center frequency of the event spectra in this instance and is defined by:

$$f_c \overset{\text{def}}{\equiv} \langle x \rangle = \frac{\int_{-\infty}^{\infty} x f(x) dx}{\int_{-\infty}^{\infty} f(x) dx} \tag{2}$$

Center frequency is an important metric due the fact that it can give an indication of whether the majority of an event's spectral content is high or low frequency in nature. Aspects of spectral content classified in this manner can give information regarding slip distance, Q determination, and other source parameters (Beresnev 2001; Brune 1970, 1971; Eaton 2011, 2014; Maxwell 2011). In this regard, we calculate center frequency for all events in the dataset and use the result as a means to classify microseismic events based on correlation with event location, pump parameters, and accompanying spectral parameters such as bandwidth.

Event Bandwidth

The bandwidth of each event was also determined in order to classify microseismic events. The global maximum of each event spectra and associated prominence was determined. From here, the width was calculated at one-half of the total prominence. As a result, there is a relative measure of overall bandwidth for each event in the dataset. Figure 3 shows an example of a

wideband event (left) as well as a narrowband event (right). Moreover, these measures were computed for windowed compressional waves, windowed shear waves, and also a combined window that captured both waveforms. The mean and standard deviation of bandwidth were computed for the three windows for all events in order to understand the overarching trend in spectral bandwidth for the different waveforms present in the data.

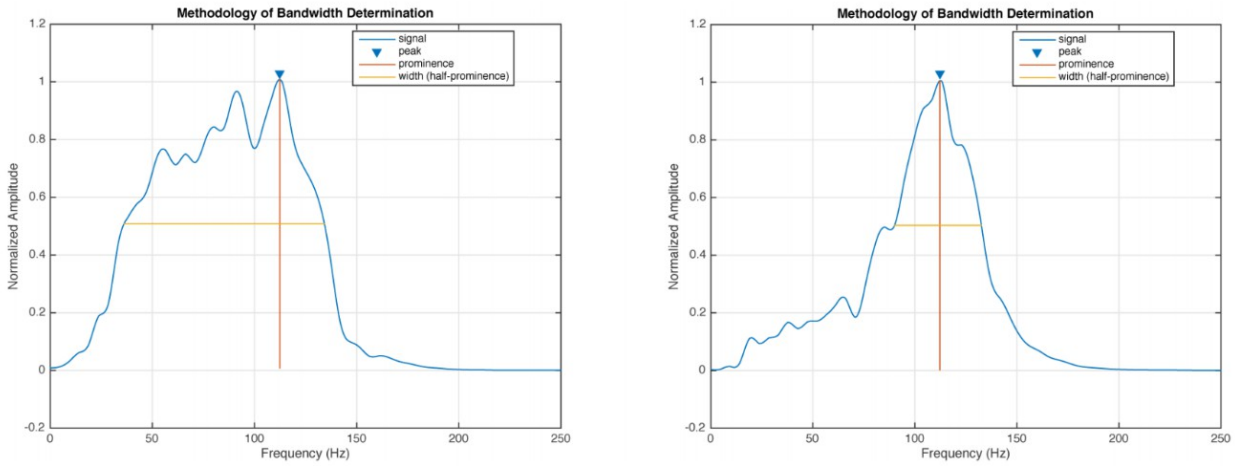

Figure 3—An example event showing how bandwidth is determined. Note that the width of the signal (horizontal line), which we call the bandwidth, is measured at one-half the prominence (vertical line)

Results

In an effort to understand the properties inherent within the event spectra, we calculated, for all events in the hydraulic fracturing process, the mean center frequency and bandwidth (Table 2). It can be seen that the windowed compressional waves have a lower mean center frequency as well as a lower mean bandwidth when compared to the windowed shear waves. Furthermore, the mean center frequency and bandwidth of the combined window is closer to that of the shear wave than the windowed compressional wave, giving an indication that the majority of microseismic content of the hydraulic fracturing process may be associated with shear openings.

Table 2—Mean values of spectral characteristics for entire dataset

	Mean Center Frequency (Hz)	Mean Bandwidth (Hz)
Compressional Wave	86.0	61.9
Shear Wave	92.3	72.5
Combined Window	88.6	66.0

After calculating the various metrics by which we hope to better understand event spectra, we began to visualize the information in order to determine if there were any immediate relationships that could be seen between spectral characteristics and process parameters. Overall,

variation in spectra can be seen from event to event, which indicates that there is also variation in the source mechanism. Figure 4a shows a spectral representation for all events in the hydraulic fracturing process. After displaying the spectra based on sorted center frequency and bandwidth measures, it can be seen that the variability now shows a representative measure of these spectral characteristics. For example, the bandwidth of the events progresses from narrowband to broadband (Figure 4b). It is important to note; however, that for narrowband events, there is still variation in where the maximum amplitude occurs. Displaying the event spectra as a function of sorted center frequency (Figure 4c), it can also be seen that the majority of broadband events are located in the middle of the image. This is due to the fact that the centroid method considers where the majority of amplitude exists within the signal. As such, broadband events have a higher likelihood of having a center frequency around the mean.

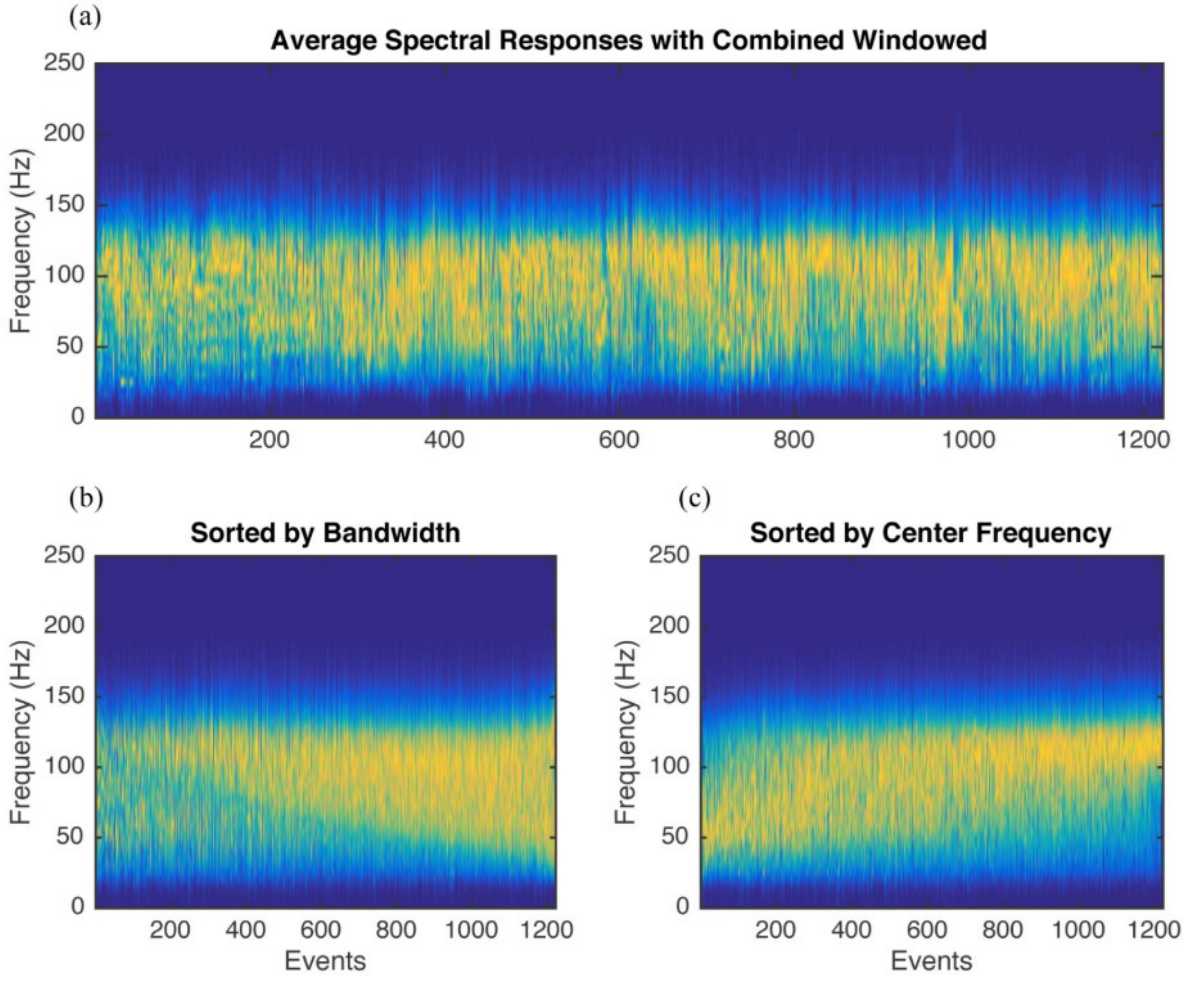

Figure 4—Event spectra of combined windowed data - horizontal axis shows event count, color encodes frequency amplitude where blue is lowest and yellow is greatest amplitude. Unsorted events (top) show that there is a range of variability in frequency response present in the data. Bandwidth-sorted spectra (bottom left) show that there is also variability of narrowband events. Center frequency- sorted events (bottom right) show that at the highest center frequencies (events 1,000 to 1200), the events are more narrowband in nature.

Going forward, scalar values of bandwidth and microseismic event magnitude, as well as process parameters - surface pressure, slurry flow rate, and proppant concentration - are plotted as a function of time (Figure 5). An interesting relation can be seen in stage 7 of the hydraulic fracturing process. Specifically, there is an inverse relationship between event bandwidth and event magnitude. This is especially evident in the last twenty minutes of the stage after proppant concentration, slurry flow rate, and finally surface pressure all drop to zero. This is an indication that narrowband events carry with them a higher magnitude.

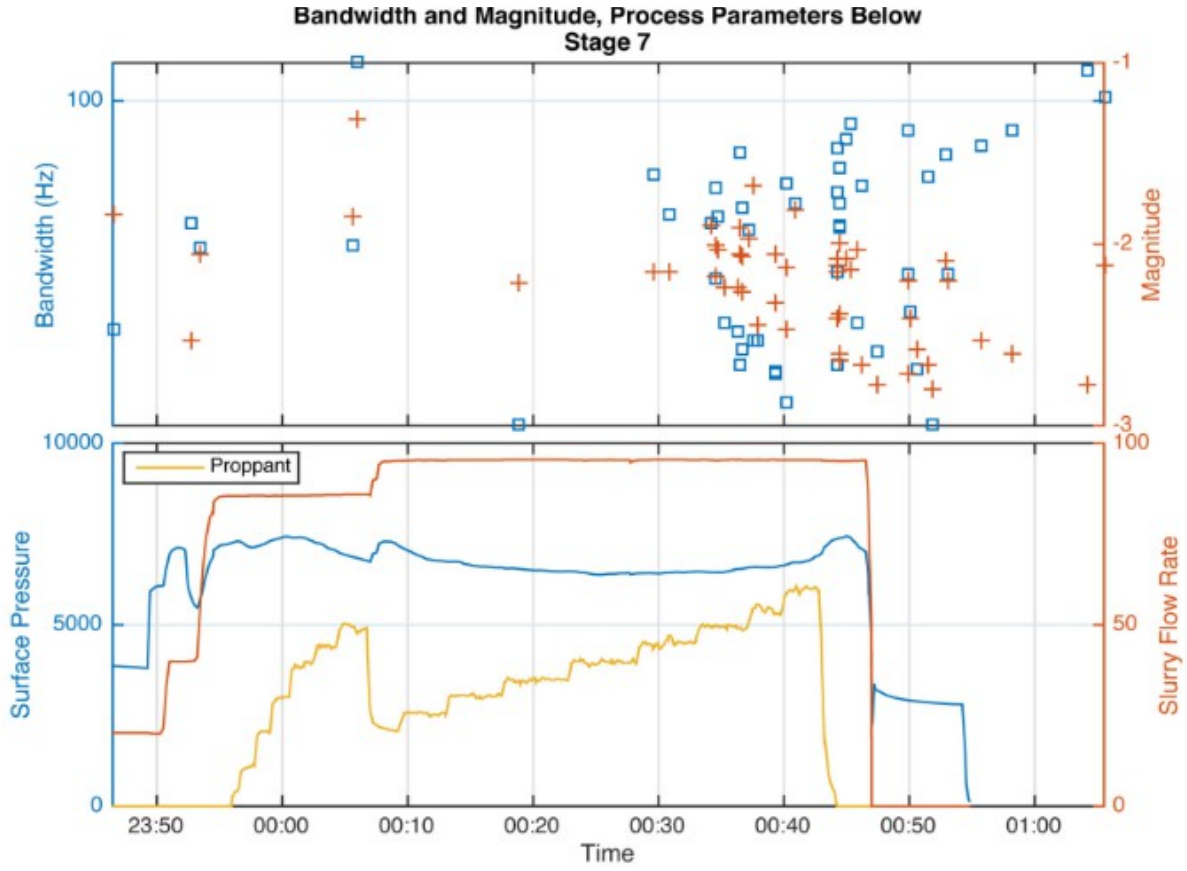

Figure 5—Bandwidth and magnitude shown as a function of time with other process parameters. The top figure shows bandwidth (blue square) and microseismic event magnitude (red plus) as a function of time. The bottom figure shows process parameters – surface pressure (blue), slurry flow rate (red), and proppant concentration (yellow). Bandwidth and event magnitude display an inverse relationship.

In order to understand the shear and compressional relation within each individual event, we consider the ratio of windowed shear wave bandwidth and windowed compressional wave bandwidth, much like the traditional S/P amplitude method. Given that the mean bandwidth and center frequency is lower for compressional waves and higher for shear waves, it is our assumption that a ratio of the shear and compressional bandwidths will give insight as to the nature of the microseismic event. In that regard, the locations of microseismic events are shown in Figure 6. Here, the size and color encode the ratio of shear and compressional wave

bandwidths. As such, events that have large S/P bandwidth ratios are potentially shear wave dominated events. Conversely, those events having a small S/P bandwidth ratio are likely dominated by compressional energy.

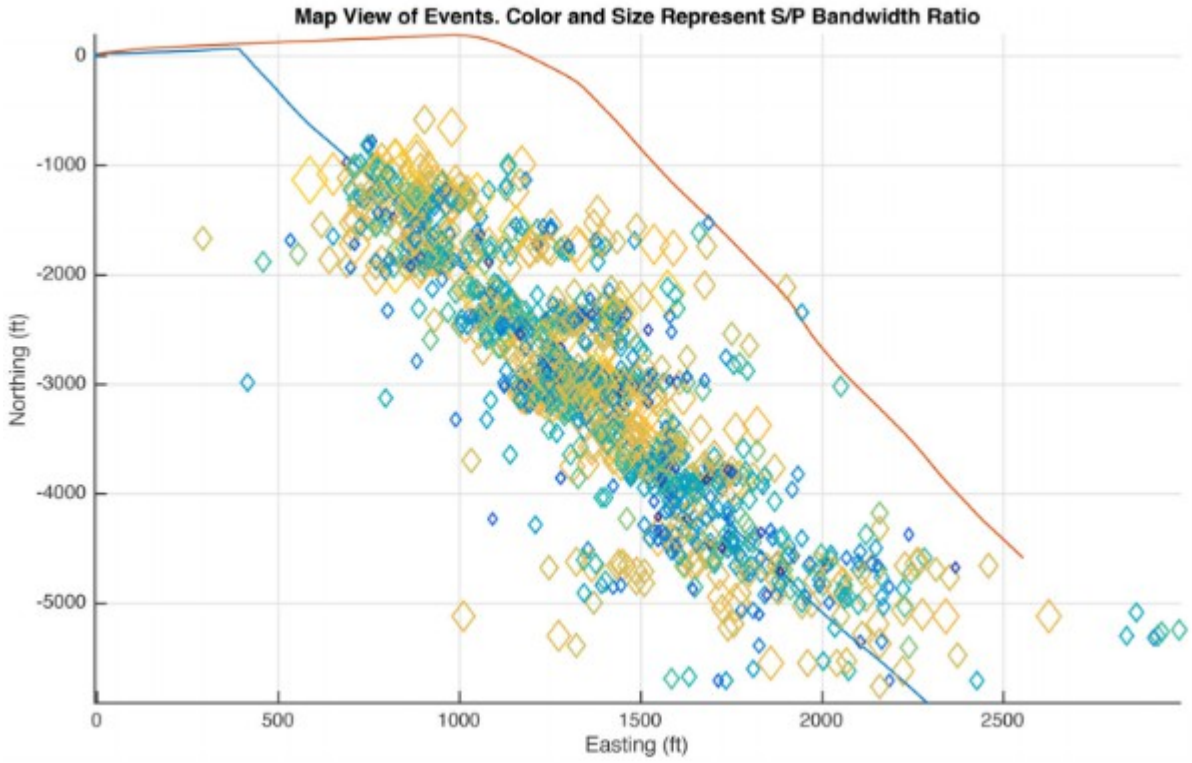

Figure 6—Map view of event locations (diamonds) for all eighteen stages of hydraulic fracturing process. As before, the treatment well is blue and the observation well is shown in red. Color and size of diamonds represent the S/P ratio of bandwidth. As such, larger yellow diamonds indicate events that have mainly shear content. Conversely, small blue diamonds represent events dominated by tensile content.

Despite the fact that only one monitoring well was used in this hydraulic fracturing process, which would lead to an inability to use traditional shear wave or compressional wave amplitude ratios, an indication of source mechanism can still be gleaned from the spectral content contained in the data. While it may be difficult to determine whether high or low shear regions exist, it may be possible to garner some knowledge regarding the fault plane (Warpinski 2010).

Conclusion

While traditional moment tensor inversion fails with the typical microseismic survey geometry, through the use of spectral analysis, characterization of microseismic events is still achievable in some regard. Even at the preliminary stages of investigation, specific relationships can be seen. For example, after finding the bandwidth of compressional and shear waveforms, it can be seen that the compressional waves are, in general, more narrowband events. Considering the ratio of shear and compressional bandwidths gives an indication of shear events in the treatment zone.

Acknowledgements

The authors would like to acknowledge support from RPSEA under contract 11122-20.

References

Bainbridge, Geoffrey S., and Gordon F. West. “A Tube Wave Damping Device For Crosshole

Seismics.” 1996 SEG Annual Meeting. Society of Exploration Geophysicists, 1996 Beresnev, Igor A. “What we can and cannot learn about earthquake sources from the spectra of seismic

waves.” Bulletin of the Seismological Society of America 91.2 (2001): 397–400 Bracewell, R. “The Fourier transform and its applications.” McGraw-Hill electrical and electronic

engineering series (1965)

Brune, James N. “Tectonic stress and the spectra of seismic shear waves from earthquakes.” Journal

of geophysical research 75.26 (1970): 4997–5009 Brune, James N. “Correction.” Journal of geophysical research 76 (1971): 5002 Daley, Thomas M., et alet al. “Tube-wave suppression in single-well seismic acquisition.” Geophysics

68.3 (2003): 863–869 Du, Jing, Ulrich Zimmer, and Norm Warpinski. “Fault Plane Solutions from Moment Tensor

Inversion for Microseismic Events using Single-Well and Multi-Well Data.” Focus (2011). Eaton, David W. “Q determination, corner frequency and spectral characteristics of microseismicity induced by hydraulic fracturing.” 2011 SEG Annual Meeting. Society of Exploration Geophysicists, 2011 Eaton, David W. “Magnitude, scaling, and spectral signature of tensile microseisms.” EGU General

Assembly Conference Abstracts. Vol. 16. 2014 Gaiser, James E., et alet al. “Vertical seismic profile sonde coupling.” Geophysics 53.2 (1988):

206–214 Maxwell, Shawn C. “What does microseismic tell us about hydraulic fracture deformation.” CSEG-

Recorder 36.8 (2011): 31–45 Mawell, Shawn. Microseismic imaging of hydraulic fracturing: Improved engineering of unconventional shale reservoirs. No. 17. SEG Books, 2014. Vavry uk, Václav. “On the retrieval of moment tensors from borehole data.” Geophysical Prospecting

55.3 (2007): 381–391 Warpinski, Norman Raymond, and Jing Du. “Source-mechanism studies on microseismicity induced by hydraulic fracturing.” SPE Annual Technical Conference and Exhibition. Society of Petroleum Engineers, 2010.